

Vanadium doping effects on microstructure and dielectric properties of barium titanate ceramics

Wei Cai ^{*}, Chunlin Fu, Zebin Lin, Xiaoling Deng

School of Metallurgical and Materials Engineering, Chongqing University of Science and Technology, Huxi Town, Shapingba, Chongqing 401331, China

Received 8 June 2011; received in revised form 8 June 2011; accepted 14 June 2011

Available online 21 June 2011

Abstract

V-doped barium titanate ceramics were prepared by conventional solid state reaction method. XRD patterns show that V^{5+} ions have entered into the tetragonal perovskite structure of solid solution to substitute for Ti^{4+} ions on the B sites. Addition of vanadium accelerates grain growth of BTO ceramics and there is abnormal grain growth of barium titanate ceramics with higher vanadium concentration. Vanadium doping can increase the Curie temperature and decrease the dielectric loss of barium titanate ceramics. As vanadium concentration increases, the remnant polarization of V-doped BTO ceramics begins to increase and reaches the maximum and then decreases. The coercive electric field for V-doped barium titanate ceramics decreases with the increasing of vanadium concentration. As temperature rises, the remnant polarization and the coercive electric field of V-doped barium titanate ceramics decrease simultaneously.

© 2011 Elsevier Ltd and Techna Group S.r.l. All rights reserved.

Keywords: B. Microstructure; C. Dielectric properties; D. Barium titanate; Vanadium; Ceramics

1. Introduction

Barium titanate ($BaTiO_3$, short for BTO) is one of the important ferroelectric materials with perovskite structure, which has been used as multi-layer ceramic capacitor (MLCC), ferroelectric random access memories (FRAM), piezoelectric sensors, optoelectronic devices, actuators, and so forth because of its excellent dielectric, piezoelectric and ferroelectric properties.

It is well known that the microstructure, dielectric and ferroelectric properties of barium titanate can be modified by a wide variety of substitutions possible at Ba^{2+} on A sites or Ti^{4+} on B sites independently or simultaneously in perovskite structure. These dopants can be isovalent or heterovalent. Effects of isovalent substitutions such as Zr^{4+} , Hf^{4+} , Mn^{4+} for Ti^{4+} and Pb^{2+} , Ca^{2+} , Sr^{2+} for Ba^{2+} on microstructure, dielectric properties and phase transition of BTO ceramics have been done [1–5]. The heterovalent substitutions such as Mg^{2+} , Dy^{3+} , Tb^{3+} , Eu^{3+} , Nd^{3+} , Gd^{3+} , Yb^{3+} , Sm^{3+} , Er^{3+} , Ho^{3+} , Sb^{3+} , Sc^{3+} , La^{3+} , Nb^{5+} , Al^{3+} , Bi^{3+} , Cu^{2+} , Cr^{3+} , Fe^{3+} , and so forth for Ti^{4+} or

Ba^{2+} cause charge imbalance and require creation of vacancies in A sites or B sites or oxygen sublattice or generation of holes to maintain electrical charge neutrality [6–20]. Li et al. [8] found that Tb-doped $BaTiO_3$ not only obtained the large dielectric constant (70,000–80,000) and the small dielectric loss (less than 4%), but also obtained good capacitance-temperature coefficient. Rejab et al. [9] found that addition of Nd can cause phase transformation from tetragonal to cubic and inhibit grain growth of barium titanate ceramics. Cernea et al. [12] prepared Ho-doped $BaTiO_3$ ceramics by sol–gel combustion method and found that the ceramics prepared from nanopowder exhibit good dielectric properties (dielectric constants of 4400–2500 at 10 Hz to 100 kHz, respectively, and at the Curie temperature $T_C = 132^\circ C$). Liu and co-workers [17] found that the doping with Ga^{3+} or tiny Al^{3+} ions shows the clear aging effect, while the high-level Al^{3+} -doping suppresses the aging effect and the suppression is mainly attributed to the kinetically limited migration of oxygen vacancies due to the lattice shrinkage. It is implied that proper doping can improve the microstructure and dielectric properties of BTO ceramics. Vanadium is one of important dopants. Noguchi and Miyayama [21] and Zeng et al. [22] reported that the B-site substitution by V^{5+} could increase the remnant polarization of $Bi_4Ti_3O_{12}$ and $CaBi_4Ti_4O_{15}$ ferroelectric ceramics, respectively. Vanadium

^{*} Corresponding author. Tel.: +86 23 65023479; fax: +86 23 65023706.

E-mail address: caiwei_cqu@163.com (W. Cai).

doping effects on dielectric properties of strontium bismuth niobate and barium strontium titanate have been studied by Nguyen and co-workers [23] and Newman and co-workers [24,25]. Cavalcante and co-workers found that addition of vanadium can reduce and broaden the maximum dielectric constant of $\text{BaZr}_{0.1}\text{Ti}_{0.9}\text{O}_3$ ceramics [26]. However, little information on the microstructure and dielectric properties of V-doped barium titanate ceramics is available. In this paper, V-doped barium titanate ceramics were prepared by conventional solid state reaction method and vanadium doping effects on microstructure, dielectric and ferroelectric properties were investigated.

2. Experimental procedures

BaTiO_3 ceramics, pure and doped with 0.5–1.5 at.% V_2O_5 , were prepared by conventional solid state reaction method. The starting raw chemicals were high purity BaCO_3 ($\geq 99.9\%$, Sinopharm Group Co. Ltd.), TiO_2 ($\geq 99.9\%$, Sinopharm Group Co. Ltd.), and V_2O_5 ($\geq 99.9\%$, Sinopharm Group Co. Ltd.) powders. BaCO_3 , TiO_2 and V_2O_5 were weighed respectively in stoichiometric proportions and were added into ball milling jar, then milled for 2 h in distilled water and zirconia media. After the slurry was dried, the mixture consisting of BaCO_3 , TiO_2 and V_2O_5 was calcined in an alumina crucible at 1100°C for 4 h in air and BaCO_3 , TiO_2 and V_2O_5 reacted to form V-doped BaTiO_3 powders. The calcined powders were remilled for 2 h and then

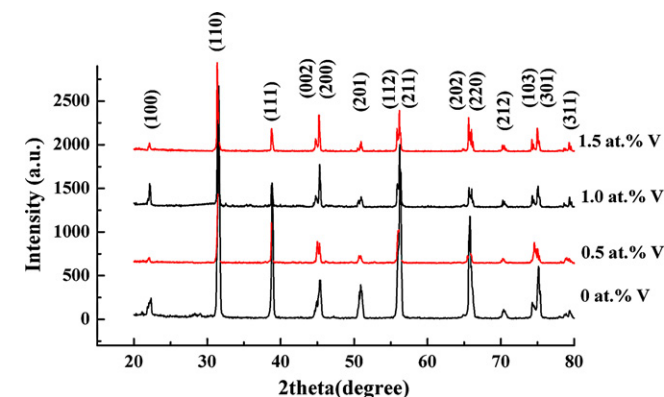


Fig. 1. XRD patterns of V-doped BTO ceramics at room temperature.

dried. The powders added with 7 wt.% binder were compacted into disk-shaped pellets with a diameter of 10.0 mm and thickness of 1.0 mm at 20 MPa pressure. The green pellets of both pure and V-doped BaTiO_3 were sintered at 1350°C for 6 h in air.

The crystal structure of the ceramic samples was examined at room temperature by X-ray diffraction (XRD, DX-2700, Dandong Fangyuan). Surface morphology of the sintered samples was examined by scanning electron microscope (SEM, S-3700 N, Hitachi).

In order to measure the dielectric and ferroelectric properties, silver paste was painted on the polished samples as the electrodes and fired at 830°C for 15 min. The capacitances of

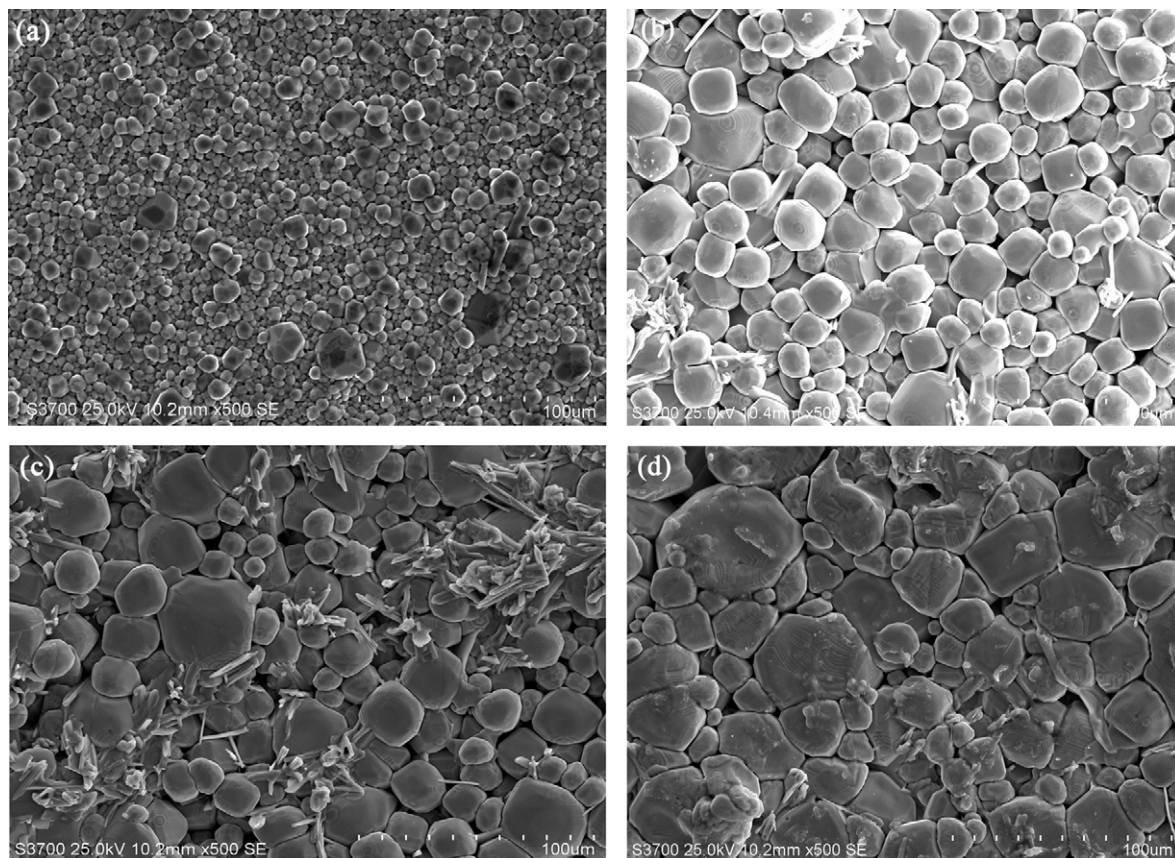


Fig. 2. SEM micrographs of BTO ceramics with different vanadium concentrations: (a) 0 at.%, (b) 0.5 at.%, (c) 1.0 at.%, (d) 1.5 at.%.

the ceramics were determined by LCR (Agilent HP 4980A) at 1 V/mm from $-60\text{ }^{\circ}\text{C}$ to $150\text{ }^{\circ}\text{C}$ with $0.5\text{ }^{\circ}\text{C}/\text{min}$. The dielectric constant was calculated from the capacitance using the following equation:

$$\varepsilon = Cd/\varepsilon_0 A \quad (1)$$

where C is the capacitance (F), ε_0 the free space dielectric constant value (8.85×10^{-12} F/m), A the capacitor area (m^2) and d the thickness (m) of the ceramics. The polarization–electric field (P – E) hysteresis characteristics were performed out using a ferroelectric test system (TF2000e, aixACCT).

3. Results and discussion

3.1. Crystal structure

Fig. 1 illustrates the XRD patterns of V-doped BTO ceramics at room temperature. It is observed that the pure and V-doped BTO ceramics are only single phase perovskite structure without the evidence of the second phase. It implies that V^{5+} ions have entered into the unit cell maintaining the perovskite structure of solid solution. According to Fig. 1, it can be seen that there are two diffraction peaks about 45° and 75° diffraction angles corresponding to $(0\ 0\ 2)/(2\ 0\ 0)$ and $(1\ 0\ 3)/(3\ 0\ 1)$ crystal faces for V-doped BTO ceramics, respectively. It indicates that the pure and V-doped BTO ceramics belong to the tetragonal system based on the X-ray diffraction pattern of barium titanate (JCPDS file no.05-0626). According to the tolerance factor equation $t = R_A + R_O/\sqrt{2}(R_B + R_O)$ (where R_A , R_B and R_O are ionic radii of an A-site cation, a B-site cation, and an oxygen ion, respectively), when V^{5+} ions ($R_{\text{V}^{5+}} = 0.054\text{ nm}$) are assumed to occupy the Ba^{2+} ions ($R_{\text{Ba}^{2+}} = 0.135\text{ nm}$) on the A sites, t is about 0.684. When V^{5+} ions are assumed to occupy the Ti^{4+} ions ($R_{\text{Ti}^{4+}} = 0.0605\text{ nm}$) on the B sites, t is about 1.002. Therefore, it is suggested that the V^{5+} ions tend to occupy B sites of the perovskite structure.

3.2. Surface morphology

Fig. 2 shows SEM micrographs of V-doped BTO ceramics. It can be found that all the sintered ceramic samples are dense. The grain size of V-doped BTO ceramics is larger than that of the pure BTO ceramics and the average grain size increases with the increasing of vanadium concentration. Addition of vanadium can accelerate grain growth. The grains of the BTO ceramics with 0.5 at.% V are homogeneous. However, when vanadium concentration is above 0.5 at.%, there is coexistence of small and large grains in V-doped BTO ceramics. It indicates that addition of vanadium leads to abnormal grain growth. As vanadium concentration increases, the number of large grain increases. The smallest and the largest grain of BTO ceramics with 1.5 at.% V are $5\text{ }\mu\text{m}$ and $68\text{ }\mu\text{m}$, respectively. According to Fig. 2(c), there are strip-shaped grains in BTO ceramics with 1.0 at.% V. The observed behavior is believed to be caused by vanadium as sintering aid. Since the melting point of vanadium pentoxide is low ($\sim 690\text{ }^{\circ}\text{C}$), vanadium pentoxide can form liquid phase in this multiple oxide system during sintering

process. When vanadium concentration is more, more liquid phase around grain can accelerate transportation of substance and finally leads to abnormal grain growth.

Fig. 3 shows the temperature dependence of dielectric properties for V-doped BTO ceramics measured at 1 kHz. The three structural transitions (cubic to tetragonal $T_{\text{C-T}}$ or T_{C} , tetragonal to orthorhombic $T_{\text{T-O}}$, orthorhombic to Rhombohedral $T_{\text{O-R}}$) can be apparently observed for V-doped BTO ceramics (shown in Fig. 3(a)). Observed temperature peaks for all structural transitions and dielectric constant values at 1 kHz for all samples are given in Table 1. Addition of vanadium leads to slight increase of T_{C} and $T_{\text{T-O}}$ and has no effect on $T_{\text{O-R}}$. The increase of T_{C} with vanadium doping can be explained by cation vacancy. V^{5+} has higher valence than Ti^{4+} , the substitution of V^{5+} for Ti^{4+} introduces cation vacancy on A-site to meet the requirement of charge neutrality. The cation vacancies on A-site could lead to an enhancement of ferroelectric structure distortion, thus resulting in a higher T_{C} [27]. From Table 1, it is also found that the maximum of dielectric constant initially decreases and then increases with the increasing of vanadium concentration. According to Fig. 3(b), the dielectric loss of V-doped BTO ceramics is lower than that of the pure BTO ceramics when the temperature is $-60\text{ }^{\circ}\text{C}$ to $120\text{ }^{\circ}\text{C}$, and the dielectric loss decreases with the increasing of vanadium concentration when the temperature is 40 – $120\text{ }^{\circ}\text{C}$. It indicates that addition of vanadium can decrease

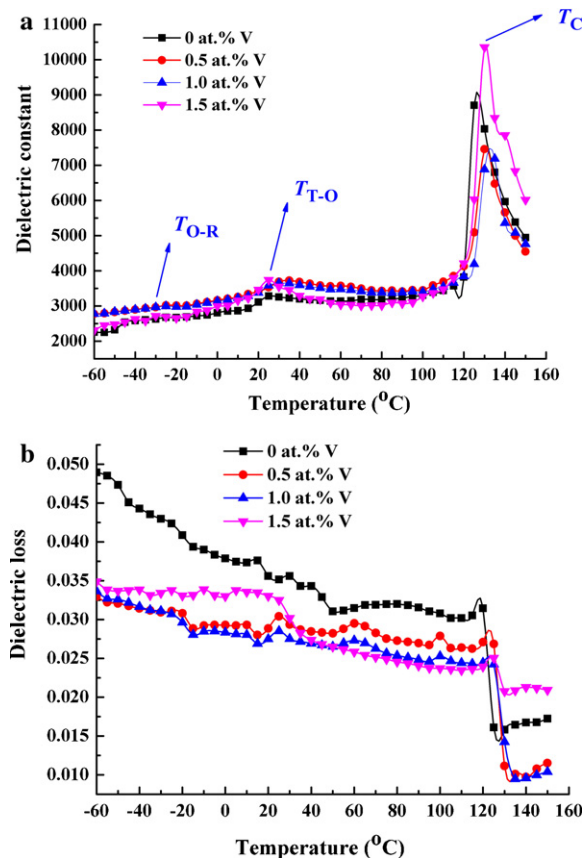


Fig. 3. The temperature dependence of dielectric properties of V-doped BTO ceramics measured at 1 kHz (a) dielectric constant– T (b) dielectric loss– T .

Table 1

Phase transition temperatures and dielectric constant values for V-doped BTO ceramics at 1 kHz.

Vanadium concentration (at.%)	T_{C-T} or T_C ($^{\circ}\text{C}$)	T_{T-O} ($^{\circ}\text{C}$)	T_{O-R} ($^{\circ}\text{C}$)	$\epsilon_{\max}(T_C)$
0	125	25	−25	8705
0.5	130	35	−25	7459
1.0	135	30	−25	7191
1.5	130	25	−25	10356

the dielectric loss of BTO ceramics. It may be due to charge compensation effect of vanadium. Ti^{4+} is chemically less stable. Ti^{4+} ion easily change into Ti^{3+} as follows: $\text{Ti}^{4+} + \frac{1}{2}\text{O}_\text{O}^\times \rightarrow \text{Ti}^{3+} + \frac{1}{2}\text{V}_\text{O}^{\bullet\bullet}$. When V^{5+} ion diffuses into BTO ceramics, the reaction is as follows: $\text{V}^{5+} + \text{Ti}^{3+} \rightarrow \text{V}^{4+} + \text{Ti}^{4+}$, V^{5+} ion restrains the reaction of Ti^{4+} to Ti^{3+} , which makes oxygen vacancy concentration less. The decrease of oxygen vacancy concentration can make the dielectric loss lower.

Fig. 4 shows dielectric constant as a function of temperature at different frequencies for V-doped BTO ceramics. The peaks of dielectric constant of the pure and V-doped BTO ceramics slightly decrease with the increasing of frequency. There is no obvious frequency dispersion around the peaks of the dielectric constant for the pure and V-doped BTO ceramics.

Fig. 5 shows hysteresis loops of BTO ceramics with different vanadium concentrations at 1 kHz. The remnant polarization

($2P_r$) of V-doped BTO ceramics begins to increase and reaches the maximum (vanadium concentration = 0.5 at.%) and then decreases as vanadium concentration increases. There are two opposite effects on remnant polarization. On the one hand, oxygen vacancies act as space charge, which causes strong domain pinning. Decrease in defect concentration leads to an increase in the remnant polarization [28]. So the restraint of oxygen vacancies due to vanadium doping brings about the increase of the remnant polarization. On the other hand, the ionic radius of V^{5+} is smaller than that of Ti^{4+} , an increasing amount of V^{5+} would lead to a reduced electronic polarization so that the remnant polarization decreases [23]. The variation of the remnant polarization with vanadium concentration may be determined by the competition of the decrease of oxygen vacancy concentration and the reduced electronic polarization. When vanadium concentration is 0–0.5 at.%, the mechanism of restraint of oxygen vacancies is dominant, so the remnant

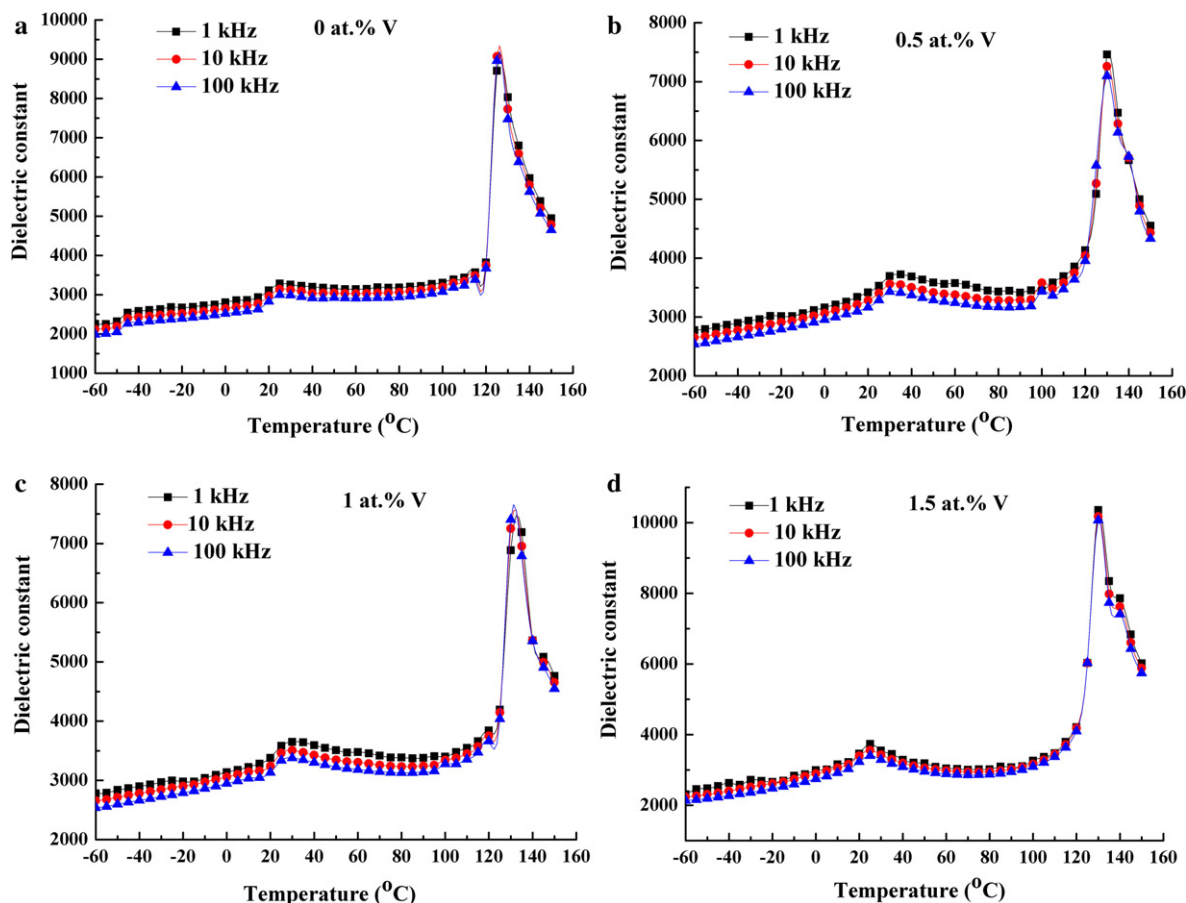


Fig. 4. Dielectric constant as a function of temperature at different frequencies for BTO ceramics with different vanadium concentrations: (a) 0 at.%, (b) 0.5 at.%, (c) 1.0 at.%, (d) 1.5 at.%.

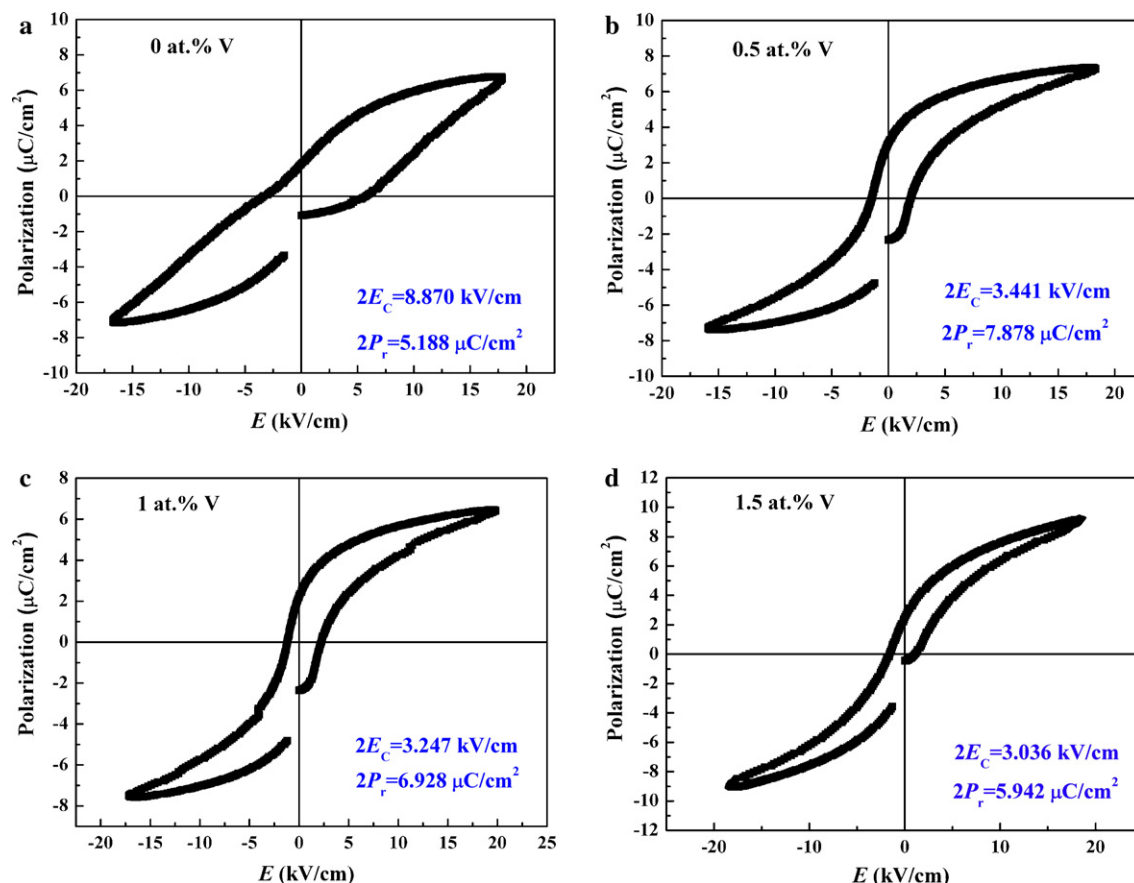


Fig. 5. Hysteresis loops of BTO ceramics with different vanadium concentrations at 1 kHz (a) 0 at.%, (b) 0.5 at.%, (c) 1.0 at.%, (d) 1.5 at.%.

polarization increases. While vanadium concentration is higher than 0.5 at.%, the reduced electronic polarization caused by vanadium doping is dominant, so the remnant polarization decreases. Moreover, the coercive electric field ($2E_C$) for V-doped BTO ceramics is significant lower than that of the pure BTO ceramics and slightly decreases with the increasing of vanadium concentration when vanadium concentration is 0.5–1.5 at.%. The decrease of the coercive electric field could be attributed to oxygen vacancy concentration and grain size of V-doped BTO ceramics. On the one hand, oxygen vacancy may affect domain wall motion by screening of the polarization charge. A formation of mechanical barriers against the domain walls by oxygen vacancies, so called domain wall pinning, might also stabilize the domain configuration [29]. As mentioned above, the addition of vanadium can decrease oxygen vacancy concentration. It indicates that as vanadium concentration increases, domain wall pinning reduces so that domain wall moves easily so as to decrease the coercive electric field. On the other hand, barrier for switching ferroelectric domain must be broken through and energy barrier decreases as grain size increases. So reversal polarization process of a ferroelectric domain is more difficult inside a small grain than in a large grain [30]. As mentioned above, the grain size of V-doped BTO ceramics increases with the increasing of vanadium concentration. Thus, the coercive electric field decreases as vanadium concentration increases.

Fig. 6 shows hysteresis loops for V-doped BTO ceramics measured at various frequencies. From Fig. 6(a)–(c), it is found that the hysteresis loops of BTO ceramics with 0–1.0 at.%V become slimmer with the increasing of frequency, which indicates that the remnant polarization and the coercive electric field decrease as frequency increases. Nevertheless, the hysteresis loop of BTO ceramics with 1.5 at.%V has no evident change as frequency increases from 100 Hz to 1000 Hz. It may be attributed to the difference of polarization mechanism. When vanadium concentration is 0–1.0 at.%, there are electron and ion displacement polarization, turning-direction polarization and space charge polarization caused by oxygen vacancy in samples. When the frequency increases from 100 Hz to 1000 Hz, the space charge polarization cannot keep up with change of electric field so that the remnant polarization and the coercive electric field decrease. As mentioned above, addition of vanadium can restrain oxygen vacancy. When vanadium concentration is 1.5 at.%, the concentration of oxygen vacancy is minimum. Space charge polarization caused by oxygen vacancy has no effect on ferroelectric properties of samples. Hence, the remnant polarization and the coercive electric field of BTO ceramics with 1.5 at.%V are almost constant with the increasing of frequency.

Fig. 7 shows hysteresis loops for V-doped BTO ceramics measured at various temperatures. The remnant polarization

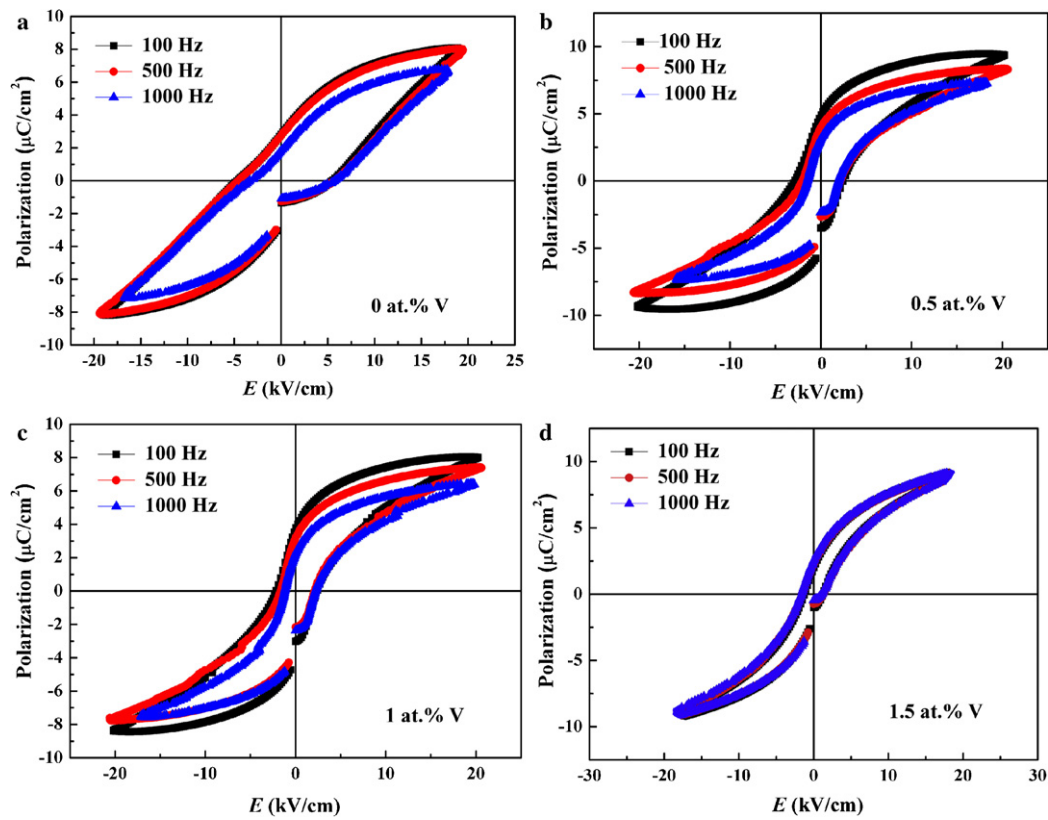


Fig. 6. Hysteresis loops of BTO ceramics with different vanadium concentrations at various frequencies (a) 0 at.%, (b) 0.5 at.%, (c) 1.0 at.%, (d) 1.5 at.%.

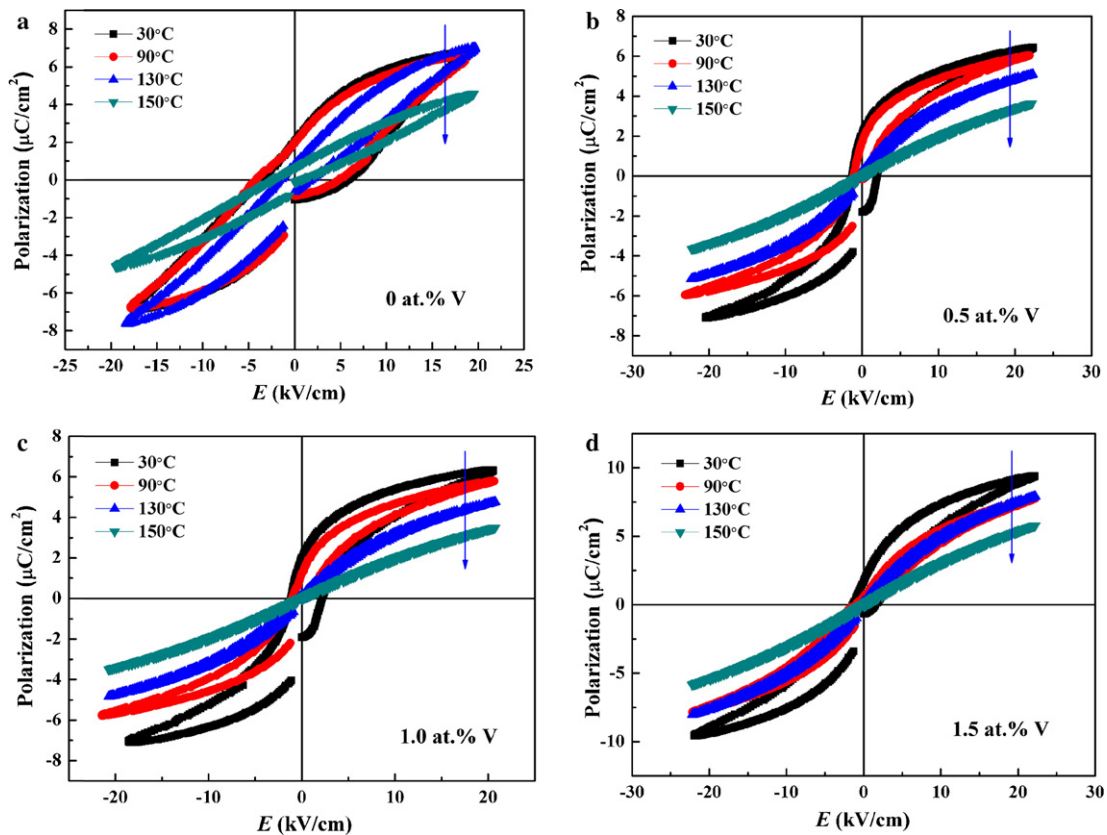


Fig. 7. Hysteresis loops of BTO ceramics with different vanadium concentrations at various temperatures (a) 0 at.%, (b) 0.5 at.%, (c) 1.0 at.%, (d) 1.5 at.% saturation polarization.

and the coercive electric field of the pure and V-doped BTO ceramics decrease simultaneously as temperature rises. It is due to phase transition from ferroelectric to paraelectric. The paraelectric phase of V-doped BTO ceramics at higher temperature is more so that the remnant polarization decreases. The domain and domain wall can switch more easily when the temperature is higher. Hence the coercive electric field decreases. When temperature is 150 °C, the hysteresis loops of BTO ceramics with 0.5–1.5 at.%V is close to straight line, which indicates that relationship of P – E is linear. However, the P – E of the pure BTO ceramics at 150 °C is nonlinear, which indicates that there is coexistence of ferroelectric and paraelectric phase when temperature is above the Curie temperature (125 °C). It may be attributed to the smaller grain size of BTO ceramics (shown in Fig. 2(a)).

4. Conclusions

BTO ceramics with different vanadium concentrations were prepared by conventional solid state reaction method. V^{5+} ions have entered into the unit cell maintaining the tetragonal perovskite structure of solid solution to substitute for Ti^{4+} ions on the B sites. Addition of vanadium can accelerate grain growth of BTO ceramics. When vanadium concentration exceeds a critical value, there is the abnormal grain growth of V-doped BTO ceramics. The Curie temperature of V-doped BTO ceramics is higher than that of the pure BTO ceramics. Vanadium doping can decrease the dielectric loss of BTO ceramics. There is no obvious frequency dispersion around the peaks of the dielectric constant for V-doped BTO ceramics. The remnant polarization of V-doped BTO ceramics begins to increase and reaches the maximum and then decreases as vanadium concentration increases. The coercive electric field for V-doped BTO ceramics is significant lower than that of the pure BTO ceramics and the coercive electric field slightly decreases with the increasing of vanadium concentration when vanadium concentration is 0.5–1.5 at.%. As temperature rises, the remnant polarization and the coercive electric field of V-doped BTO ceramics decrease simultaneously.

Acknowledgements

This work was supported financially by the Natural Science Foundation Project of CQ CTTC (grant no. CSTC2010BB4286 and 2011BA4027), Research Foundation of Chongqing University of Science and Technology (grant no. CK2010Z05) and the Science and Technology Research Project of Chongqing Education Committee of Chongqing, China (grant no. KJ101415).

References

- [1] W. Cai, C.L. Fu, J.C. Gao, H.Q. Chen, Effects of grain size on domain structure and ferroelectric properties of barium zirconate titanate ceramics, *Journal of Alloys and Compounds* 480 (2009) 870–873.
- [2] M.R. Panigrahi, S. Panigrahi, Synthesis and microstructure of Ca-doped $BaTiO_3$ ceramics prepared by high-energy ball-milling, *Physica B* 404 (2009) 4267–4272.
- [3] H.T. Langhammer, T. Müller, K.H. Felgner, H.P. Abicht, Crystal structure and related properties of manganese-doped barium titanate ceramics, *Journal of the American Ceramic Society* 83 (2000) 605–611.
- [4] S. Anwar, P.R. Sagdeo, N.P. Lalla, Study of the relaxor behavior in $BaTi_{1-x}Hf_xO_3$ ($0.20 \leq x \leq 0.30$) ceramics, *Solid State Sciences* 9 (2007) 1054–1060.
- [5] J.C. Chen, Y. Zhang, C.S. Deng, X.M. Dai, Crystallization kinetics and dielectric properties of barium strontium titanate based glass-ceramics, *Materials Chemistry and Physics* 121 (2010) 109–113.
- [6] W. Cai, C.L. Fu, J.C. Gao, C.X. Zhao, Dielectric properties and microstructure of Mg doped barium titanate ceramics, *Advances in Applied Ceramics* 110 (2011) 181–185.
- [7] S.H. Yoon, S.H. Kwon, K.H. Hur, Dielectric relaxation behavior of acceptor (Mg)-doped $BaTiO_3$, *Journal of Applied Physics* 109 (2011) 084117.
- [8] Y.X. Li, X. Yao, X.S. Wang, Y.B. Hao, Studies of dielectric properties of rare earth (Dy,Tb,Eu) doped barium titanate sintered in pure nitrogen, *Ceramics International* (2011), doi:10.1016/j.ceramint.2011.04.042.
- [9] N.A. Rejab, S. Sreekantan, K.A. Razak, Z.A. Ahmad, Structural characteristics and dielectric properties of neodymium doped barium titanate, *Journal of Materials Science: Materials in Electronics* 22 (2011) 167–173.
- [10] S.K. Jo, J.S. Park, Y.H. Han, Effects of multi-doping of rare-earth oxides on the microstructure and dielectric properties of $BaTiO_3$, *Journal of Alloys and Compounds* 501 (2010) 259–264.
- [11] V.V. Mitic, Z.S. Nikolic, V.B. Pavlovic, V. Paunovic, M. Miljkovic, B. Jordovic, L. Zivkovic, Influence of rare-earth dopants on barium titanate ceramics microstructure and corresponding electrical properties, *Journal of the American Ceramic Society* 93 (2010) 132–137.
- [12] M. Cernea, C. Galassi, B.S. Vasile, P. Ganea, R. Radu, G. Ghita, Electrical investigations of holmium-doped $BaTiO_3$ derived from sol–gel combustion, *Journal of Materials Research* 25 (2010) 1057–1063.
- [13] M.M. Vijatović Petrović, J.D. Bobić, T. Ramoška, J. Banys, B.D. Stojanović, Antimony doping effect on barium titanate structure and electrical properties, *Ceramics International* (2011), doi:10.1016/j.ceramint.2011.04.015.
- [14] M.C. Ferrarelli, C.C. Tan, D.C. Sinclair, Ferroelectric, electrical, and structural properties of Dy and Sc co-doped $BaTiO_3$, *Journal of Materials Chemistry* 21 (2011) 6292–6299.
- [15] K. Niesz, T. Ould-Ely, H. Tsukamoto, D.E. Morse, Engineering grain size and electrical properties of donor-doped barium titanate ceramics, *Ceramics International* 37 (2011) 303–311.
- [16] Y. Yuan, S.R. Zhang, X.H. Zhou, B. Tang, Effects of Nb_2O_5 doping on the microstructure and the dielectric temperature characteristics of barium titanate, *Journal of Materials Science* 44 (2009) 3751–3757.
- [17] Y.Y. Guo, M.H. Qin, T. Wei, K.F. Wang, J.M. Liu, Kinetics controlled aging effect of ferroelectricity in Al-doped and Ga-doped $BaTiO_3$, *Applied Physics Letters* 97 (2010) 112906.
- [18] N. Kumada, H. Ogiso, K. Shiroki, S. Wada, Y. Yonesaki, T. Takei, N. Kinomura, Rising T_c in Bi and Cu co-doped $BaTiO_3$, *Materials Letters* 64 (2010) 383–385.
- [19] H.T. Langhammer, T. Müller, R. Böttcher, H.P. Abicht, Structural and optical properties of chromium-doped hexagonal barium titanate ceramics, *Journal of Physics: Condensed Matter* 20 (2008) 085206.
- [20] M. Unruan, T. Sareein, J. Tangsritrakul, S. Prasertpalichat, A. Ngamjar-urojana, S. Anata, R. Yimnirun, Changes in dielectric and ferroelectric properties of Fe^{3+}/Nb^{5+} hybrid-doped barium titanate ceramics under compressive stress, *Journal of Applied Physics* 104 (2008) 124102.
- [21] Y. Noguchi, M. Miyayama, Large remanent polarization of vanadium-doped $Bi_4Ti_3O_{12}$, *Applied Physics Letters* 78 (2001) 1903–1905.
- [22] J.T. Zeng, Y.X. Li, Q.B. Yang, Q.R. Yin, Ferroelectric and piezoelectric properties of vanadium-doped $CaBi_4Ti_4O_{15}$ ceramics, *Materials Science and Engineering B* 117 (2005) 241–245.
- [23] Y. Wu, C. Nguyen, S. Seraji, M.J. Forbess, S.J. Limmer, T. Chou, G.Z. Cao, Processing and properties of strontium bismuth vanadate niobate ferroelectric ceramics, *Journal of the American Ceramic Society* 84 (2001) 2882–2888.
- [24] S.J. Liu, V.Y. Zenou, I. Sus, T. Kotani, M.V. Schilfgaarde, N. Newman, Structure-dielectric property relationship for vanadium- and scandium-doped barium strontium titanate, *Acta Materialia* 55 (2007) 2647–2657.

- [25] S. Bandyopadhyay, S.J. Liu, Z.Z. Tang, R.K. Singh, N. Newman, Leakage-current characteristics of vanadium- and scandium-doped barium strontium titanate ceramics over a wide range of DC electric fields, *Acta Materialia* 57 (2009) 4935–4947.
- [26] F. Moura, A.Z. Simões, L.S. Cavalcante, M.A. Zaghete, J.A. Varela, E. Longo, Ferroelectric and dielectric properties of vanadium-doped $\text{Ba}(\text{Ti}_{0.96}\text{Zr}_{0.10})\text{O}_3$ ceramics, *Journal of Alloys and Compounds* 466 (2008) L115.
- [27] Y. Noguchi, M. Miyayama, T. Kudo, Direct evidence of A-site-deficient strontium bismuth tantalate and its enhanced ferroelectric properties, *Physical Review B* 21 (2001) 4102–4106.
- [28] Y. Noguchi, I. Miwa, Y. Gosshima, M. Miyayama, Defect control for large remanent polarization in bismuth titanate ferroelectrics—doping effect of higher-valent cations—, *Japanese Journal of Applied Physics* 39 (2000) L11259.
- [29] W. Cai, C.L. Fu, J.C. Gao, X.L. Deng, Effect of Mn doping on the dielectric properties of $\text{BaZr}_{0.2}\text{Ti}_{0.8}\text{O}_3$ ceramics, *Journal of Materials Science: Materials in Electronics* 21 (2010) 317–325.
- [30] C.C. Leu, C.Y. Chen, C.H. Chien, M.N. Chang, F.Y. Hsu, C.T. Hu, Domain structure study of $\text{SrBi}_2\text{Ta}_2\text{O}_9$ ferroelectric thin films by scanning capacitance microscopy, *Applied Physics Letters* 82 (2003) 3493–3495.